Sutardi, T., Wang, L., Paul, M. C. and Karimi, N. (2018) Numerical simulation approaches for modelling a single coal particle combustion and gasification. Engineering Letters, 26(2), pp. 257-266.

http://eprints.gla.ac.uk/163247/

Numerical Simulation Approaches for Modelling a Single Coal Particle Combustion and Gasification

Tata Sutardi, Linwei Wang, Manosh C. Paul, and Nader Karimi

Abstract - Combustion and gasification are the fundamental processes of coal utilization, and the research of these applications has been continuously progressing. Numerical modelling is one of the methodologies that also has significant advancement, due to the progress of computational engineering and also considering economic impact. This paper is a part of the numerical developments on the coal combustion and gasification that introduces a new approach by which a single coal particle model has been developed and used to investigate those processes. CFD (Computational Fluid Dynamics) techniques with an Eddy Break Up (EBU) model and also with a set of kinetics parameter reactions are used in the study. However, defining the chemical reactions is crucial for the model development. Seven reactions for coal combustion and additional six reactions for gasification are investigated. It is identified that the best fit kinetic parameter value for the pre-exponent factor (A) of R2 and R3, while comparing with the experimental results, is 20 and 1000, respectively. Finally, these values are implemented into the model of both coal particle combustion and gasification for investigation. The results of the simulation show that the H_2 and CH_4 products from the gasification are significantly higher than those from the combustion. The maximum mole fraction value of CO products in combustion is ~ 1.5 times higher than in gasification at an air condition, which is unexpected. However, CO production lasted longer than ~ 200 ms at O_2 condition below than 21% in the coal gasification, which resulted in more CO production. These results clearly identify the process of coal combustion and gasification. This particle model can thus be considered for further investigation for various coal combustion and gasification applications.

Keywords: Combustion, gasification, numerical model, kinetics parameter.

I. INTRODUCTION

Coal continues to be the largest fuel used for the electricity generation worldwide based on the IEO (International Energy Outlook) report published in 2016 [1]. Coal accounted for 40% of the total electricity generation in 2012 and will decline to 29% in 2040 despite a continued increase in the total capacity for the electricity generation from 8.6 trillion kWh in 2012 to 10.6 trillion kWh in 2040 [1]. The total capacity however from coal-fuel in 2040 is predicted to be 23% above the 2012 baseline in total [2]. Moreover, coal could also be utilized through gasification process either for electricity generation or chemical stocks [3]. And the way to utilize coal through the gasification is expected to be environmental friendly and cleaner.

All authors are member of Systems, Power & Energy Research Division, School of Engineering, University of Glasgow, Glasgow, G12 8QQ, UK.

The first author, Tata Sutardi, is a PhD student at the University of Glasgow and engineer in the Agency for assessment and application of technology (BPPT)-Indonesia.

The second author, Linwei Wang, is also a PhD student at the University of Glasgow.

The third author, Dr Manosh C. Paul BSc (H) MSc PhD FHEA CEng MIMechE, is a Reader in Thermofluids, and Deputy Head of Mechanical Engineering. He is also the corresponding author of this paper. (E-mail address: Manosh.Paul@glasgow.ac.uk ; Tel.: +44 (0) 141 3308466)

The final author, Dr Nader Karimi, is a Lecturer in Mechanical Engineering.

Furthermore, since both the processes of combustion and gasification would still be dominant in the next few decades as evidenced by the published reports [1], the research and development in these fields are therefore expected to grow continuously. While the power generation from a coal combustion plant is the key objective, resulting emissions in the gas products are avoidable. On the other hand, gasification results in the production of syngas which could be utilised for downstream application to generate power and heat/cooling with more environmental friendly.

Coal combustion involves oxidation of char and also coal volatile, while gasification is a partial oxidation process by which coal is converted to gases called syngas containing CO, H_2, CH_4, and CO_2. Importantly, gasification process occurs at different stages e.g. oxidation, pyrolysis and reduction [4]. Therefore, the reaction mechanisms for coal gasification could be developed by the inclusion of pyrolysis and reduction reactions from combustion [5].

However, one of the important factors for developing these reaction mechanisms to be used in numerical simulation is their kinetic parameters. The values of the kinetic parameters presented in [6] were obtained through an experimental procedure. However, several other literatures showed a quite significant difference in these values for the reaction mechanisms [7]. Incidentally, the values of the kinetic rate for these reactions found to converge to a range that can be considered acceptable [8]. Therefore, in most of the kinetic expressions, the exponents of species' concentrations are not equal to the appropriate stoichiometric coefficient. Moreover, the process of combustion and gasification consists of several reactions and they occur simultaneously, a kinetic rate of each reaction has a contribution to the whole rate of reaction mechanisms. It is important to obtain a proper value of all the kinetic parameters that could produce the results best compared to those of experiment. Hence, the validation procedures will be the important key of this research.

This paper focuses on the development of computational simulation for coal particle combustion and gasification. As highlighted above, the kinetic parameter has an important role on performing the simulation and their value is specific for each reaction [7]. Applying several set of kinetic parameters reaction into the simulation may not directly provide any suitable results. Therefore, identifying the proper kinetic parameter is necessary in order to obtain an agreement between the result of simulation and experiment. This paper is principally focused on this objective with an approach that is going to be termed as "numerically identification approach" to identify the kinetic parameters of the chosen reactions with validation performed at the stage of combustion. The authors also recently developed and applied another approach by which the kinetic parameters could be identified and further details are presented in [9]. The result to be presented in the paper is expected to contribute to a better understanding of the processes describing the thermochemical behaviour of coal combustion and gasification.

II. MODEL DEVELOPMENT

The single coal particle combustion and gasification processes occur in the drop tube furnace (DTF). Computational physical geometry of the furnace is illustrated in Fig. 1[10]. The DTF is represented by a cylindrical shape geometry as illustrated in Fig. 1(a), with the inlet diameter of 7 cm, and the hot wall furnace length of 25 cm from the inlet. The coal particle injection starts from the centre of the inlet. The axi-symmetric model with a grid distribution used for the simulation can be seen in Fig. 1(b).
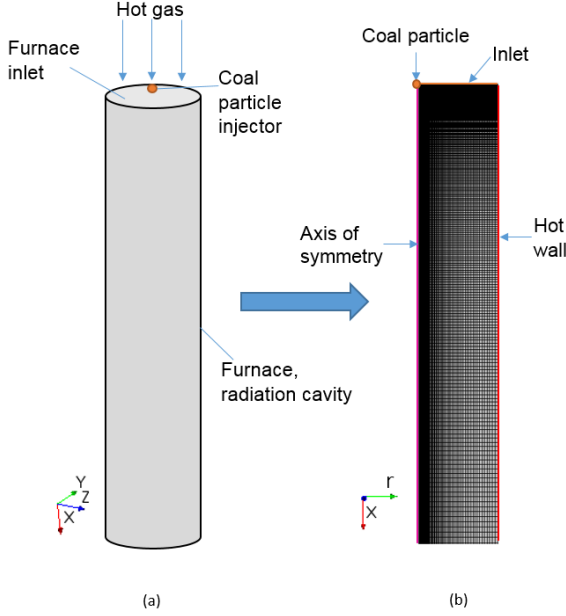

Fig. 1.An illustration of the geometry model, (a) cylindrical shape and (b) axi-symmetric model with grid

The coal particle combustion simulations are conducted under a quiescent gas condition (inactive flow) and the quiescent gas condition is set by turning off the gas flows a few seconds prior to the particle injection [11]. These procedures are based on the procedures of the experimental simulation [10, 12], and then the reactions of simulation as shown in the TABLE I are applied [13].

TABLE I
COAL COMBUSTION AND GASIFICATION REACTIONS

No	Mechanism	Enthalpy (kJ/mol)
R1	Raw coal $\rightarrow$ YYCoal volatile + (1-YY) Char	
R2	$C + O_2 \rightarrow CO_2$	-393
R3	$C + 0.5O_2 \rightarrow CO$	-111
R4	$C + CO_2 \rightarrow 2CO$	+172
R5	$C + H_2O \rightarrow CO + H_2$	+131
R6*	$C + 2H_2 \rightarrow CH_4$	-75
R7	Coal Volatile + $O_2 \rightarrow CO_2 + H_2O + N_2$	
R8	$CO + 0.5O_2 \rightarrow CO_2$	-283
R9*	$H_2 + 0.5O_2 \rightarrow H_2O$	-242
R10*	$CO + H_2O \rightarrow CO2 + H_2$	-41
R11*	$CH_4 + H_2O \rightarrow CO + 3H_2$	+206
R12*	$CH_4 + 0.5O_2 \rightarrow CO + 2H_2$	-36
R13*	$CH_4 + CO_2 \rightarrow 2CO + 2H_2$	+247

*the reactions included in gasification

In the simulation model, seven reactions are used for representing the coal combustion/oxidation processes and another six reactions are added for the gasification mechanisms. The R1, R2, R3, R4, R5, R7, and R8 are reactions for coal combustion, then another inclusion of R6, R9, R10, R11, R12, and R13 to perform the gasification.

Eddy Break Up (EBU) with a kinetic parameter model is used for controlling the chemical reaction mechanisms. For the particle transport and transformation, a Lagrangian approach with multi-phase method is used, as the coal particle consists of several components (raw coal, char, coal volatile, H_2O, and ash content).

The mechanisms of the coal particle conversion / interaction with the gas inside the reactor are described through the several equations as follows.

The continuity equation of raw coal component in particle p is described as

$$\frac{dm_{cp}}{dt} = -R_{cp} , \qquad (1)$$

where the net rate for raw coal consumption is given by

$$R_{cp} = k_1 \alpha_{cp} m_p . \qquad (2)$$

And the rate of production for coal volatile is described as

$$R_{cv} = k_1 YY \alpha_{cp} m_p . \qquad (3)$$

Then, the reaction rate coefficient is the Arrhenius form given by

$$k_1 = AT^\beta exp \left(\frac{-E_a}{R_c T} \right). \qquad (4)$$

Particle and gas reactions begin after the volatile fraction of raw coal particle completely evolved. This heterogeneous reaction rate is determined by combining the effect of the Arrhenius rate and diffusion coefficient, and for this case the constant diffusion coefficient is assigned as 4.5E-5 m²/s. The model of particle rate consumption is then determined by

$$R_p = \frac{dm_p}{dt} = -\frac{k_m k}{k+k_m} \emptyset C_g M_w A_p , \qquad (5)$$

where,

$$k_m = \frac{(S_h)(D_m)}{d} . \qquad (6)$$

The reaction rate of each of the gas and gas (homogeneous) reactions is a function of the composition and rate constant, given by the expression:

$$R_j = R_{i,kin} = -k_j \prod_{all\ reactants} \left(\frac{\rho Y_i}{M_i} \right)^{p_{ij}}. \qquad (7)$$

The equation of motion for the particle is defined as,

$$m_p \frac{d\overline{u_{i,J,k}^p}}{dt} = \sum \bar{F}. \qquad (8)$$

The effect of gravity force has been used in this simulation since these forces influence the parameter of investigation.

A. Governing equation

In the reacting flow, the changes of pressure, temperature, velocity, and species concentration are the results of the interaction among the fluid flow, molecular transport, heat transfer and chemical reaction. In order to consider these effects on the simulation models, a set of mathematical modelling, which consists of the Navier–Stokes, mass continuity, species mass conservation and energy conservation equations, is developed.

The law of mass conservation results in the mass continuity equation as shown below:

$$\frac{\partial \rho}{\partial t} + \frac{\partial(\rho u_x)}{\partial x} + \frac{\partial(\rho u_r)}{\partial r} + \frac{\rho u_r}{r} = 0 \tag{9}$$

The equation for the conservation of axial momentum is represented by [14]:

$$
\begin{aligned}
\frac{\partial(\rho u_x)}{\partial t} &+ \frac{1}{r}\frac{\partial(r\rho u_x u_x)}{\partial x} + \frac{1}{r}\frac{\partial(r\rho u_r u_x)}{\partial r} \\
&= -\frac{\partial p}{\partial x} \\
&+ \frac{1}{r}\frac{\partial}{\partial x}\left[r\mu\left(2\frac{\partial u_x}{\partial x} - \frac{2}{3}(\nabla\cdot\vec{u})\right)\right] \\
&+ \frac{1}{r}\frac{\partial}{\partial r}\left[r\mu\left(\frac{\partial u_x}{\partial r} - \frac{\partial u_r}{\partial x}\right)\right] + \rho g_x
\end{aligned}
\tag{10}
$$

And, for the radial momentum conservation:

$$
\begin{aligned}
\frac{\partial(\rho u_r)}{\partial t} &+ \frac{1}{r}\frac{\partial(r\rho u_x u_r)}{\partial x} + \frac{1}{r}\frac{\partial(r\rho u_r u_r)}{\partial r} \\
&= -\frac{\partial p}{\partial r} \\
&+ \frac{1}{r}\frac{\partial}{\partial x}\left[r\mu\left(\frac{\partial u_r}{\partial x} - \frac{\partial u_x}{\partial r}\right)\right] \\
&+ \frac{1}{r}\frac{\partial}{\partial r}\left[r\mu\left(2\frac{\partial u_r}{\partial r} - \frac{2}{3}(\nabla\cdot\vec{u})\right)\right] \\
&- 2\mu\frac{u_r}{r^2} + \frac{2}{3}\frac{\mu}{r}(\nabla\cdot\vec{u})
\end{aligned}
\tag{11}
$$

where, $\nabla\cdot\vec{u} = \frac{\partial u_x}{\partial x} + \frac{\partial u_r}{\partial r} + \frac{u_r}{r}$, and ρg_x is the gravitational body force.

The concentration of each species can be expressed in terms of the mass fraction $m_i(x, r, t)$, or using the concentration of species $C_i = m_i\rho$, which is defined as the mass of species per unit volume.

The conservation law of chemical species is represented as [14],

$$\frac{\partial}{\partial t}(\rho m_i) + \nabla\cdot(\rho m_i \vec{u} + J_i) = R_i \tag{12}$$

Where R_i accounts for the production or consumption rate of the species in chemical reactions.

The energy equation in this simulation may be written as:

$$\frac{\partial(\rho E)}{\partial t} + \nabla\cdot(\vec{u}(\rho E + p)) = -\nabla\cdot\left(\sum_i h_i J_i\right) \tag{13}$$

In this simulation, the equation state of gas in the reaction is treated as ideal gas. This equation is needed to connect the thermodynamic variables such as, $p, \rho,$ and T. The ideal gas equation is expressed as

$$\frac{p}{\rho} = R_c T \tag{14}$$

R_c is the universal gas constant.

In turbulent flows, all transport processes are enhanced by turbulent fluctuations. Turbulence causes large fluctuations in mass fractions, temperature, density, velocity, and moreover extinction can occur when turbulence effects are strong. Turbulent flows are characterized by the presence of a wide range of time and scales at which motion and fluctuations take place.

In this simulation, RANS (Reynolds-Averaged Navier-Stokes) approach is used for solving the turbulence effect on the species transport. The equation describes the behaviour of the time-averaged flow quantities instead of the exact instantaneous values. In this approach, RANS equations arise when the Reynolds decomposition is implemented into the Navier-Stokes equations, and the additional Reynolds stresses introduced into those equations are then modelled through the Boussinesq hypothesis depending strongly on the turbulence kinetic energy, k, and its rate of dissipation, ϵ, which are obtained from the realizable $k - \varepsilon$ model. The transport equation for the turbulent kinetic energy may be represented as

$$
\begin{aligned}
\frac{\partial(\rho k)}{\partial t} + div(\rho k \vec{u}) &= div\left[\left(\mu + \frac{\mu_t}{\sigma_k}\right)grad\ k\right] + G_k \\
&- \rho\varepsilon
\end{aligned}
\tag{15}
$$

while, the transport equation for the viscous dissipation (the rate at which the kinetic energy of small scale fluctuation is converted into heat by viscous friction) is represented as,

$$
\begin{aligned}
\frac{\partial(\rho\varepsilon)}{\partial t} + div(\rho\varepsilon\vec{u}) &= div\left[\left(\mu + \frac{\mu_t}{\sigma_\varepsilon}\right)grad\ \varepsilon\right] \\
&+ C_{\varepsilon 1}P_k\frac{\varepsilon}{k} - C_{\varepsilon 2}\rho\frac{\varepsilon^2}{k}
\end{aligned}
\tag{16}
$$

In this simulation the constants used for the equation above are: $C_{\varepsilon 1} = 1.44$; $C_{\varepsilon 2} = 1.9$; $\sigma_k = 1$; $\sigma_\varepsilon = 1.2$

B. Simulation Procedures and Boundary conditions

The initial boundary conditions were taken from an experimental study [10, 12]. The furnace was heated up with hot air before the injection of the coal particle. The inlet condition was set as a velocity inlet, with an initial temperature of hot air of 1200K, and at the same time, the furnace wall temperature was set at 1400K. The inlet air with a velocity of 0.045 m/s was injected through the furnace's inlet until the flow became fully developed and steady-state. Additionally, to accommodate the full development region, the furnace wall was extended to 75 cm and it was set as an isolator.

In the simulations, a type of coal namely PSOC 1451 was used, identified as bituminous coal. The chemical properties of these coals were taken from the proximate and ultimate analyses, presented in TABLE II. [10].

TABLE II.
COAL CHEMICAL COMPOSITIONS

	PSOC 1451
Proximate Analysis as receives	
Moisture (%)	2.5
Volatile matter (%)	33.6
Fixed Carbon (%)	50.6
Ash (%)	13.3
Ultimate Analysis (dry basis)	
Carbon (%)	71.9
Hydrogen (%)	4.9
Oxygen (%) (by diff.)	6.9
Nitrogen (%)	1.4
Sulphur (%)	1.4
Sodium (%)	0.06
Ash (%)	13.7
Heating value dry fuel (MJ/kg)	31.5

In this simulation, defining the raw coal particle and coal volatile composition was needed because it affects the equilibrium condition of reaction. Based on the proximate and ultimate correlations, the coal volatile composition for PSOC 1451 was defined as $CH_{2.7}O_{0.248}N_{0.058}$ or the *YY* value of 0.29 as stated in the reaction balance equation R1[15].

III. MODEL VALIDATION

The simulation was developed based on the experimental procedures [10, 12] as mentioned in the previous section. The initial stage of coal combustion, i.e. the devolatilization process (R1) reaction, is stated in TABLE I. And the validation of this initial process was performed based on the results derived from the two software CFD simulations, Ansys [16, 11] and StarCCM [15, 5], since no experimental data on this stage was available in the experimental paper. The comparison result can be seen in Fig. 2, which shows the rate of coal particle mass reduction in the devolatilization process occurring prior to combustion. The coal volatile release from the coal particle causes the particle mass decreasing with time. The results from the two software present a good agreement of the mass rate of particle. It thus indicates that the application of the kinetic parameter into the devolatilization reaction worked properly in the simulation model. This initial test result was only used for the consideration of kinetic parameter before being applied in the more complex combustion reactions.
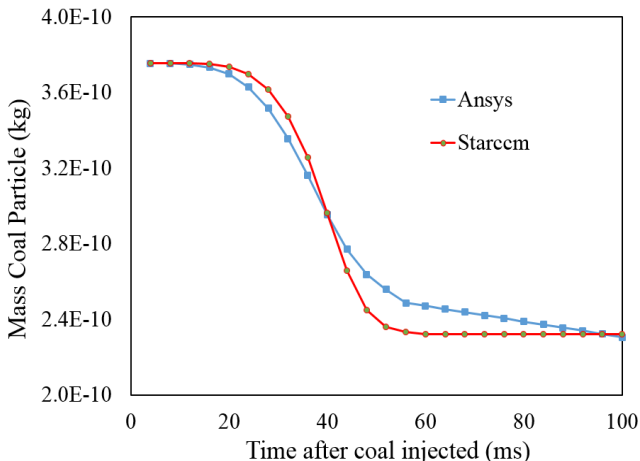

Fig. 2 The devolatilization process comparison

Further validation with the experimental result of coal particle combustion is presented in the section below considering two approaches. The first approach considers the kinetics parameter value from several reference sources, while the second approach considers the kinetic parameter through numerical identification using StarCCM CFD software.

A. Selecting kinetic parameters from reference sources

The initial study [9] indicates that the most significant mechanisms in the process of combustion are the char reactions (R2 and R3). However, more than two variations of the kinetic parameters of R2 and R3 were reported in [7]. This paper considers only the minimum and maximum values, and the detail investigation of this method was provided in other paper [9]. The values can be seen in TABLE III.

TABLE III
THE KINETIC PARAMETER VALUE

No	Kinetic parameters			Ref.
	A (unit vary)	*Ea* (j/kmol)	*β*	
R1	3.12E+05	7.40E+07	0	Alganash et.al [17]
R2	0.002	7.90E+07	0	Alganash et.al [17]
	11000	1.13E+08	0	Boiko et.al [18]
R3	0.052	1.33E+08	0	Alganash et.al [17] & Silaen [19]
	85500	1.40E+08	0.84	Watanabe et.al [20]
R4	4.4	1.62E+08	1	Alganash et.al [17] & Silaen [19]
R5	1.33	1.47E+08	1	Alganash et.al [17], Silaen [19], Howard [21]
R7	2.12E+11	2.03E+08	0	Alganash et.al [17]
R8	1.30E+11	1.26E+08	0	Alganash et.al [17], Howard [21]

The kinetic parameters outlined in TABLE III are applied into the simulation model. The simulation is developed by using the R2 value, which refers to the simulation done by Alganash et.al [17] while the R3 value refers to the simulation done by both Alganash et.al [17] and Silaen et.al [19]. The simulation is named as Simulation 1. The second simulation model developed by using R2 of Alganash et.al [17] and R3 of Watanabe et.al [20] is Simulation 2. The parameters used to compare the results between the simulations and experiment are the ignition delay time (t_{id}), the char burning out time ($_{char}$), the coal volatile burning out time (t_{cv}), maximum temperature of coal volatile combustion (T_{cv}), and maximum temperature of char combustion (T_{char}).

The results of experiments, Simulation 1, and Simulation 2 with their parameters comparison can be seen in Fig. 3.
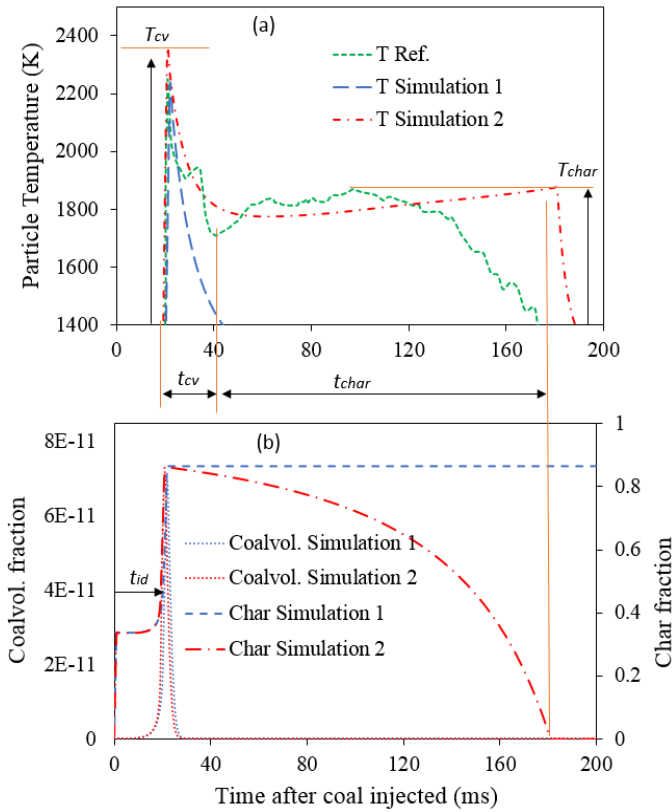
Fig. 3. The simulation result by applying the value from literature

The results of Simulation 1, represented by the blue line in Fig. 3(a) and Fig. 3(b), show the temperature and char mass fraction profiles, respectively. The temperature shows that the coal particle increases rapidly to ~2200 K (T_{cv}) within ~20 ms after coal is injected, which indicates a good agreement for the ignition delay time (t_{id}) and the maximum temperature of coal volatile combustion (T_{cv}) with the experimental result. After this point, the particle temperature of experimental result initially drops but increases again from ~40 ms. Whereas, the particle temperature of Simulation 1 (the blue line) continues to drop after having reached the maximum temperature. The char fraction of Simulation 1, however, after the same point (~40 ms), remains stable at a value of around 0.85. And the temperature drop indicates the absence of char combustion in the result of Simulation 1.

Simulation 2 is developed in order to improve the results of Simulation 1. This paper provides the kinetic parameter value of R3 as the maximum value among all the values in the literature [7]. The result of Simulation 2 shows a good agreement for the maximum of T_{cv}, T_{char}, t_{id}, t_{cv}, and t_{char} as can be seen in Fig. 3(a) and (b). The results indicate that the set of kinetic parameters of Simulation 2 can be considered for this model application as the model obtains the valid results which are comparable with the experiment. A summary comparing these results from Simulation 1, Simulation 2 and experiment is given in TABLE IV

TABLE IV
COMPARISON RESULT OF FIRST APPROACH

Parameter	Experimental	Simulation 1	Simulation 2
T_{cv} (K)*	2250	2240	2340
T_{char} (K)**	1870	Not burning	1876
t_{id} (ms)	20	20	20
t_{cv} (ms)	20	20	20
t_{char} (ms)	140	Not burning	140

*deviation [10] ~116 K
**deviation [10] ~59 K

The results presented in TABLE IV affirm that Simulation 2 has the best fit agreement with the experimental result. This result indicates that the set of kinetic properties of Simulation 2 are valid and can be considered for further investigation.

B. Selecting kinetic parameter by numerical identification approach

The kinetic parameter value of each of the reactions affects the reaction rate, as it is expressed in equation (4). The variation of kinetic parameter causes the variation of kinetic rate reaction value. In TABLE III, the minimum and maximum values of the kinetic parameters of R2 and R3 are shown. The value indicates the gap between the minimum and maximum of the kinetic rate *(k)* for R2 and R3. This space, can be numerically identified and represented as a set of the kinetic parameters value for R2 and R3, and then be applied into the simulation model. This can be an optional method for finding the best set of values of the kinetic parameters. The gap of the kinetic rates for R2 and R3 listed in TABLE III can be seen in Fig. 4

Fig. 4 (a) shows the gap of kinetic rate of R2 and (b) shows that the gap is filled by another kinetic rate from several settings of kinetic parameter values. There is possibility that more set of value could be added. However, this paper serves only three sets of value as to provide a brief description of this approach. They are called as R2-A, R2-B, and R2-C. Applying the same procedure on R3, a gap can be seen in Fig. 4(c), and additional kinetic rates are put into the gap as seen in Fig. 4(d). The additional kinetic rates are from the approach of the numerical identification of kinetic parameter value. The set of kinetic parameter values for both reactions are outlined in TABLE V [5].

TABLE V
IDENTIFYING KINETIC PARAMETER APPROACH

Reaction ID	Kinetic Parameter		
	A (unit vary)	E_a (j/kmol)	*β*
R2-A	0.004	7.9.E+7	0
R2-B	0.01	7.9.E+7	0
R2-C	20	7.9.E+7	0
R3-A	40	1.33E+08	1
R3-B	150	1.33E+08	1
R3-C	1000	1.33E+08	1

TABLE V shows another three additional set of kinetic parameters that are obtained through the numerical identification to find the best fit result of validation.
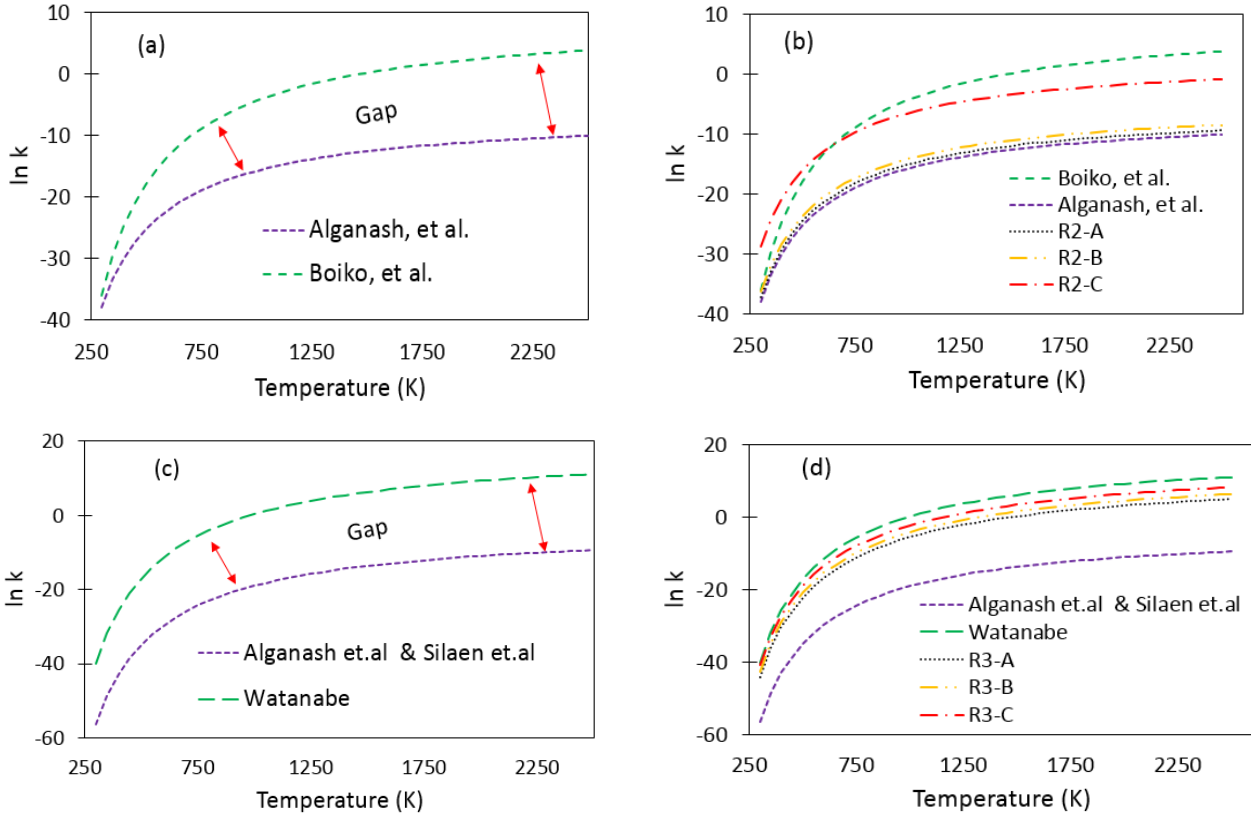
Fig. 4 The kinetic rate (k) represented in logarithmic function for (a) and (b) R2; and (c) and (d) R3

The first and second letters of reaction IDs are used to identify the reaction number, in this case they are R2 and R3. The letter A, B, and C represents the variation of each reaction number. A to C is a gradual increment of pre-exponent factor (A) that causes gradual increment of the kinetic rate value, particularly in their range of reactor temperature (1200 – 2500 K). The kinetic parameter values produce the kinetic rate values based on the Arrhenius equation. They fill the gap between the minimum and maximum value of kinetic rate from the reference sources as seen in Fig. 4.

After confirming the set of kinetic parameters in the range of kinetic rate value, based on the reference sources, each of them is implemented into the simulation model. This paper provides three variations of simulation, they are defined as simulation A, simulation B and simulation C. The simulation A uses R2-A and R3-A; the simulation B uses R2-B and R3-B; and finally the simulation C uses R2-C and R3-C for their kinetic parameter value of R2 and R3. The simulation results can be seen in Fig.5

Fig.5 shows comparison result of simulation A, B, and C with the reference/experimental result. The increment of kinetic rate of R2 and R3 from A to C, produces the increment of char reaction rate. This can be seen in Fig.5 (b), which shows the decreasing of t_{char} from A to C. The char burn out time decreases because of the char reaction occurring faster and consequently, producing more heat in a certain of time. This causes the increment of T_{char}, from A to C as can be seen in Fig.5 (a). In Figure 5, Simulation C is indicated as the best fit result, which agrees with the experimental result. Hence, the kinetic parameter value of Simulation C can be considered for further development of this numerical simulation.
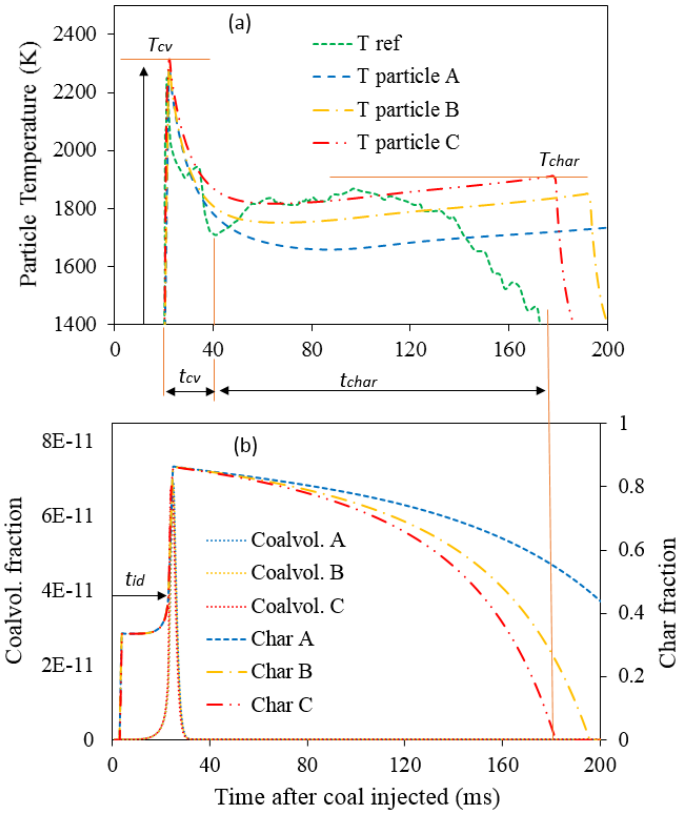

Fig.5. The simulation result by identifying kinetic parameter

As a summary, TABLE VI shows the comparison of each simulation with the experimental result.

TABLE VI
COMPARISON RESULT OF SECOND APPROACH

Parameter	Experimental	Sim. A	Sim. B	Sim. C
T_{cv} (K)*	2250	2280	2290	2313
T_{char} (K)**	1870	1736	1834	1901
t_{id} (ms)	20	20	20	20
t_{cv} (ms)	20	20	20	20
t_{char} (ms)	140	>200	154	140

*deviation [10] ~116 K
**deviation [10] ~59 K

C. Result comparison of the approaches

The best fit results of both the approaches are needed to be compared for further applications in this paper. For this purpose, some parameters are used in the comparison, and the result can be seen in Fig. 6.
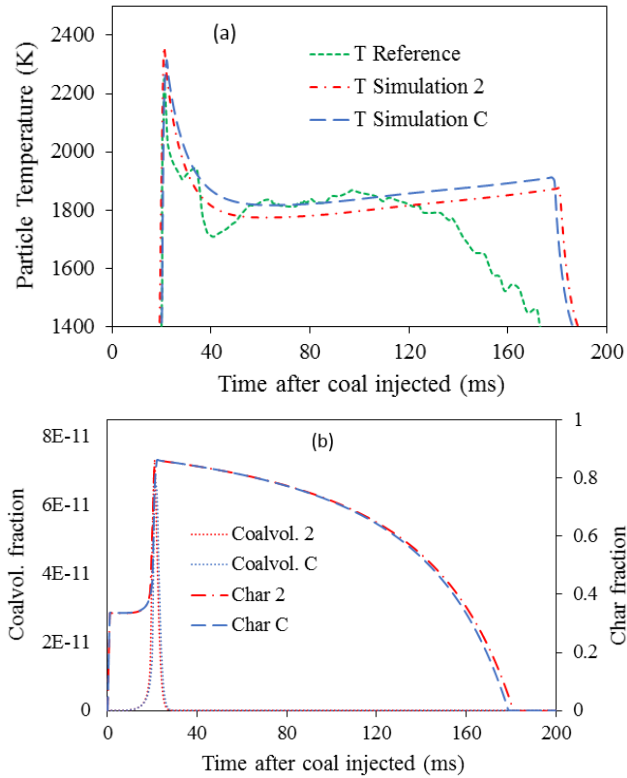

Fig. 6. The comparison result of the methods, (a) Particle temperature, (b) Coal volatile and char fraction

Fig. 6(a) shows the comparison of each method and they are compared to the experimental result as a reference. This figure shows that for T_{cv}, Simulation C is slightly closer to the experimental result. However for T_{char}, Simulation 2 is closer. But, these results are still in the acceptable range as stated in the experiment [10, 12]. Fig. 6(b) shows the comparison of the best fit results of each method, and the char and volatile matter show a good agreement. The parameter of t_{id}, t_{cv}, and t_{char} of both the results are similar and also acceptable based on the tolerance specified in the experimental result [10, 12].

Since both the methods produced the similar results, and also agree with the experimental results, they can be considered for coal combustion and further application of coal particle gasification. However, as aforementioned, this paper only focusses on one method for describing this process behaviour, i.e. the numerical identification approach. This approach is selected due to its flexibility. The wide range of coal classifications is the reason in taking this approach.

IV COMPARISON RESULTS OF COAL COMBUSTION AND GASIFICATION

This section provides the model application of a single coal particle combustion and gasification. The results of this model simulation will be used to investigate the coal combustion and gasification process. As previously mentioned, the gasification process is a further inclusion of the chemical reactions in the combustion stage, as defined in TABLE I. The parameters used in this investigation are coal volatile, CO, H_2, CO_2, and H_2O.

A. Coal volatile and H_2O gas comparison

The simulation results of coal volatile matter and H_2O as the products of coal combustion and gasification can be seen in Fig. 7.
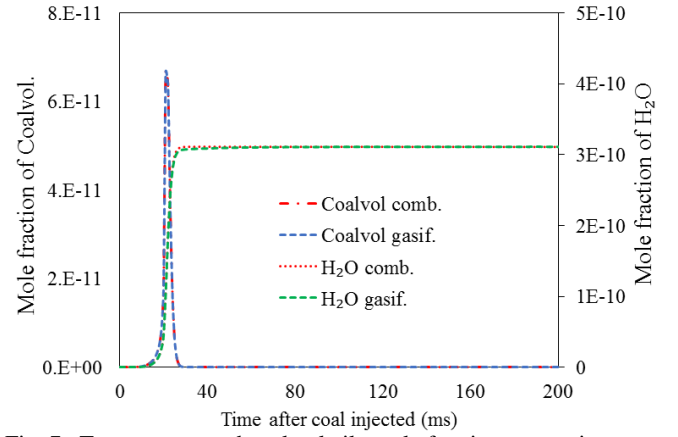

Fig. 7. Temperature and coal volatile mole fraction comparison

Fig. 7 shows that the coal volatile and H_2O products of the single coal combustion and gasification are similar. There is a slightly difference occurring before the stabilized condition of H_2O and also the peak of the coal volatile gasification slightly becomes higher than that of combustion. Nonetheless, they are relatively small and can be disregarded.

B. H_2 and CH_4 gas comparison

The simulation results between H_2 and CH_4 of a single coal combustion and gasification can be seen in Fig. 8. This figure shows that H_2 in the gasification is higher compare to the combustion. This result affirms the gasification process can be improved better on H_2 production. For CH_4 products, there are only obtained in the gasification process since the formation is not defined for the combustion reactions.
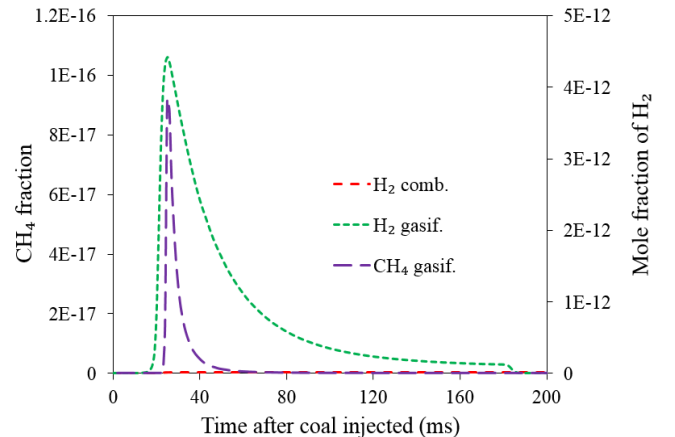

Fig. 8. The H_2 and CH_4 comparison

C. CO and CO_2 gas comparison

The simulation results between CO and CO_2 as a product of single coal combustion and gasification can be seen in Fig. 9.
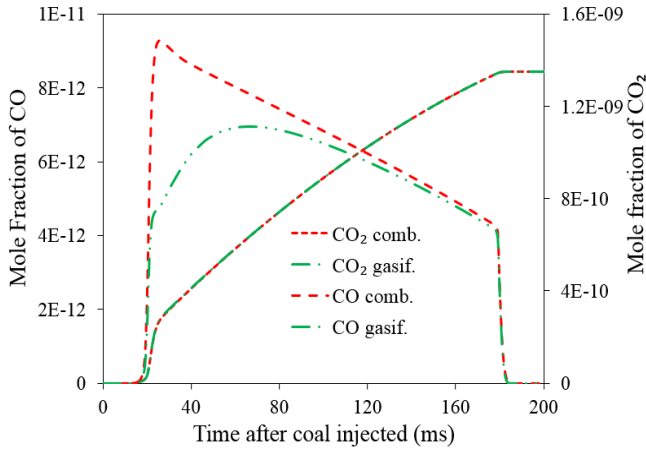

Fig. 9. The CO and CO_2 comparison

Fig. 9 shows that there is a significant difference between CO in the combustion and gasification process. In this case, the CO of gasification is lower than the CO of combustion. This result is unexpected since the gasification requires more CO and less CO_2 in their products. Hypothetically, it is occurred because of the excess oxygen condition inside the reactor. To test whether this hypothesis is true, further gasification simulations with reduced oxygen concentration are developed. The updated results of CO_2 and CO can be seen in Fig. 10.
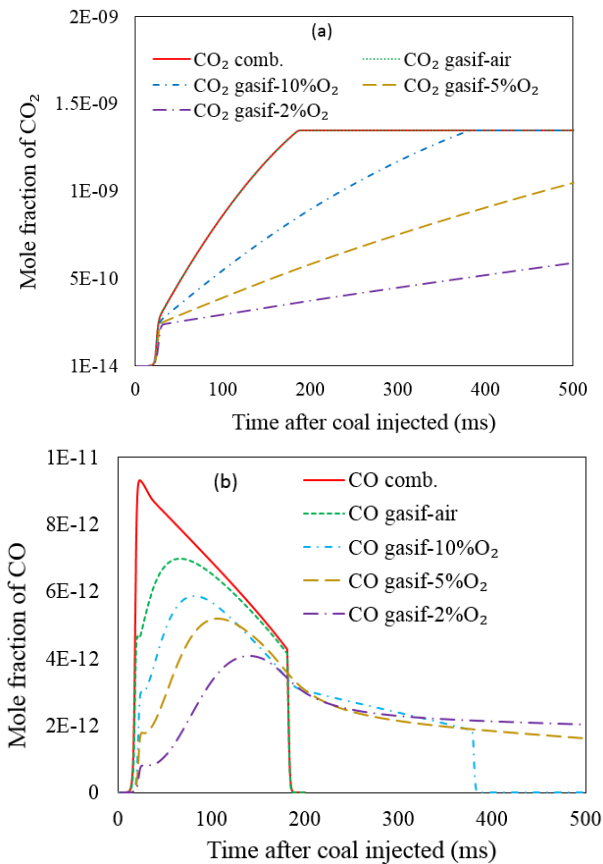

Fig. 10. The gas products under oxygen variation (a) CO_2 (b) CO

Fig. 10(a) shows that the CO_2 products of gasification decreased after the reduction of oxygen concentration inside the reactor. This reduction is expected to occur in the gasification process. Fig. 10(b) shows how the CO production lasts longer after the oxygen reduction. More CO will be obtained when the production time lasts longer. This condition is expected on the gasification process. Overall, Fig. 10 informs the importance of the oxygen control in the gasification process.

V DISCUSSION

The simulation results show a single coal particle combustion and gasification behaviour inside the reactor. In general, their behaviours align with the several sources/literatures on coal combustion and gasification. The coal particle model provides more description on the thermochemical behaviour of coal combustion and gasification.

The model describes a single coal particle combustion, thus representing the lean combustion condition. As it can be seen in the combustion behaviour, the coal particle burnt out time is at ~180 ms, and later decayed. The combustion process occurred in this period, initiated by the coal devolatilization, which on this process the coal volatile matter fraction was released from the coal and burning out. The coal volatile matter burnt out time is at ~20 ms after coal injection, lasted for ~ 10-20 ms. The char starts burning at ~30-40 ms after coal injection, lasted for ~140 ms.

The gas products of combustion appeared since the coal volatile combustion occurred, and for the CO_2 they keep increasing until the total coal particle burnt out. The CO increased at the initial of char burning, which then decreased and decayed after the coal particle burnt out. It indicated that CO is converted to be CO_2 in this process. The H_2O increased until the coal volatile burnt out, and later stabilized. The H_2 products increased after the coal volatile combustion, and decreased at the same rate as the decreasing of char or CO in the reactor. It indicates that the CO and H_2 formation is affected by the char reactions.

The coal particle gasification in this simulation occurs at the excess oxygen condition. The gasification reactions as they are defined in the model of simulation can be confirmed occurred. The process of CO_2 and H_2O formation of gasification process is similar to the combustion process. There are significant differences on the CO, H_2 and CH_4. The CO product of gasification process is less than the CO products of combustion, and it is unexpected. This condition occurred since the excess oxygen potentially converted the CO into the CO_2. This affirms the importance of controlling the oxygen concentration in the gasification process. The further model application shows how CO can be produced by reducing the oxygen concentration in the reactor. At this condition, the char reactions lasted longer by the decreasing of oxygen concentration. The H_2 production in the gasification is higher than in the combustion, and this condition is expected. The H_2 products come from the H_2O that is produced in the reaction. This insight could potentially be the main reason of increasing H_2O fraction in producing more H_2. Finally, the CH_4 is seen to be produced in the gasification process. This indicates the defined reaction work on producing CH_4 of gasification process.

VI CONCLUSION

The single coal particle model of combustion and gasification has been developed and considered for developing a better process of coal combustion and gasification. This model could be considered to estimate the burn out time of pulveriser coal combustion, which affects the design of a chamber/reactor. In the gasification application, this model can be considered to develop better gas products formation by identifying the control parameter that affects the process.

The model of simulation has identified the best fit kinetic parameter that can be used for modelling the PSOC 1451 coal type for further application. This method/approach also can be considered for other coal type application.

The simulation results show the comparison process of coal combustion and gasification. It can also be used to develop better understanding of the process mechanisms.

The gasification process is expecting lower CO_2, and the simulation shows the importance of controlling the oxygen supply for better gasification products.

The results presented above are initial information based on the model simulation. It is considerable to be applied on further investigation of coal combustion and gasification.

NOMENCLATURE

Roman Symbol

A	Pre- exponential factor (unit vary)
A_p	Surface area of particle (m^2)
C_g	Reactant gas concentration (kmol/kg)
C_i	Concentration of species (kg/m^3)
D_m	Diffusion coefficient (m^2/s)
E	Energy sources (J)
E_a	Activation Energy (J/kmol)
F	External force (N)
g	Gravity (m/s^2)
G_k	Generation of turbulence kinetic energy due to buoyancy
M_i	Molecular weight of species i
M_w	Molecular weight of solid reactant
R_c	Gas universal constant (J/kmol K)
Y_i	Mass fraction of species i
k	Kinetic energy dissipation
k_i	Kinetic rate coefficient for i
k_m	Mass transfer coefficient
m	Mass fraction
R_i	Rate exponent of reacting species
h	Enthalpy (kJ/kg)
J_i	The flux of species i
S_m	Source of mass (kg)
S_h	Sherwood number
T	Temperature (K)
YY	Mass stoichiometric coefficient
M	Mass of particle (kg)
p	Pressure (Pa)
r	Radial displacement (m)
$C_{\varepsilon1}$; $C_{\varepsilon2}$	Model constant
t	Time (s)
x	Axial displacement (m)
u	Velocity (m/s)
t_{id}	Ignition delay time
t_{cv}	Coal volatile burnt out time

t_{char}	Char burn out time
T_{cv}	Maximum temperature coal volatile combustion (K)
T_{char}	Maximum temperature char combustion (K)

Greek Symbol

α_i	Mass fraction of coal/particle component
β	Temperature exponent
τ_{ij}	Stress tensor
$\emptyset$	Ratio of stoichiometric of solid and gas
ρ	Density (kg/m^3)
ρg_i	Gravitational body force
μ	Viscosity (kg/m.s)
σ	Turbulent Prandtl number
δ	Kronecker delta

Subscript

p	Particle
c	Coal component
i, j	Species or phase
t	Turbulent
vm	Volatile matter
k	Turbulent kinetic energy (m^2/s^2)
ε	Turbulent dissipation rate (m^2/s^3)

ACKNOWLEDGEMENTS

REFERENCES

[1] DOE/EIA, (2016)"*International Energy Outlook 2016*,"In: *US Energy Information Administration,* vol. 0484,

[2] W. E. Council, 2013 "*World Energy Resource - 2013 Survey*," in *Report - Survey, ISBN : 978 0 946121298,* ed, p. 1.2.

[3] D. Yang, Sheng, Y and Green, M., (2014)"*UCG: Where in the world,*"In: *The Chemical Engineer (872),* vol. 38-41.ISSN 0302-0797.,

[4] M. L. d. Sauza-Santos, (2004)"*Solid Fuels Combustion and Gasification,*"In: *Texbook and Reference Books, . ISSN 0-8247-0971-3,*

[5] T. Sutardi, M. C. Paul, N. Karimi, and P. L. Younger, "Numerical Modelling for Process Investigation of a Single Coal Particle Combustion and Gasification," in *Lecture Notes in Engineering and Computer Science: Proceedings of The World Congress on Engineering 2017, July 5-7, 2017, London, U.K,* pp. 946-951.

[6] J. Ballester and S. Jiménez, (2005)"*Kinetic parameters for the oxidation of pulverised coal as measured from drop tube tests,*"In: *Combustion and Flame,* vol. 142, pp. 210-222,

[7] A. Zogala, (2014)"*Ctitical Analysis of Underground Coal Gasification Models. Part II: Kinetic and Computational Fluid Dynamics Models,*"In: *Journal of Sustainable Mining,* pp. 13(1), 29-37,

[8] P. Atkins, (2001)"*Chemia fizyczna [Physical chemistry],*"In: *Warszawa: PWN,*

[9] T. Sutardi, M. C. Paul, and N. Karimi, (2018)"*Investigation of Coal Particle Gasification Process with Application Leading to Underground Coal Gasification,*"In: *On Process for Submission,*

[10] Y. A. Levendis, J. Kulbhushan., K. Reza, and A. F. Sarofim, (2011)"*Combustion behavior in air of single particles from three different coal ranks and from sugarcane bagasse,*"In: *Combustion and Flame,* vol. 158, pp. 452-465,

[11] L. W. Wang, N. Karimi, and M. C. Paul, (2016)"*Numerical Study of Single Coal Particle Combustion In O2/N2 and O2/CO2 Atmospheres,*"In: *HEFAT Conference,*

[12] T. Maffei, R. Khatami, S. Pierucci, T. Faravelli, E. Ranzi, and Y. A. Levendis, (2013)"*Experimental and modeling study of single coal particle combustion in O2/N2 and Oxy-fuel (O2/CO2) atmospheres,*"In: *Combustion and Flame,* vol. 160, pp. 2559-2572,

[13] A. Żogała and T. Janoszek, (2015)"*CFD simulations of influence of steam in gasification agent on parameters of UCG process*,"In: *Journal of Sustainable Mining,* vol. 14, pp. 2-11,

[14] O. Zikanov, (2012. ISBN :978-81-265-3497-5)"*Essential Computational Fluid Dynamics,*"In: *Texbook and Reference Books, Wiley-India Edition,*

[15] R. R. Piyush Thakre, (2010)"*Setting up Coal Combustion in STARCCM+5.04,*"In:

[16] ANSYS, (2009)"*Ansys Fluent 12.0 Theory Guide.,*"In:

[17] B. Alganash, M. C. Paul, and I. A. Watson, (2015)"*Numerical investigation of the heterogeneous combustion processes of solid fuels*,"In: *Fuel,* vol. 141, pp. 236-249,

[18] E. A. Boiko, & Pachkovskii, S.V.A. , (2004)"*Kinetic Model of Thermochemical Transformation of Solid Organic Fuels.,*"In: *Russian Journal of Applied Chemistry, 77(9),* pp. 1547–1555.,

[19] A. Silaen, & Wang, T. , (2010)"*Effect of turbulence and devolatization models on coal gasification simulation in entrained-flow gasifier.,*"In: *International Journal of Heat and Mass Transfer, 53(9-10),* pp. 2074-2091.,

[20] H. Watanabe, & Otaka, M. , (2006)"*Numerical simulation of coal gasification in entrained flow coal gasifier.,*"In: *Fuel, 85(12-13),* pp. 935–943.,

[21] W. G. Howard JB, Fine DH. Fine., (1973)"*Kinetics of carbon monoxide oxidation in postflame gases*,"In: *Proceedings of 14th symposium (Int.) on combustion,* vol. p. 975–86.,